BMC Oral Health

https://doi.org/10.1186/s12903-026-09562-2

Article in Press

Comparison of mid-palatal suture morphology via suture bone densities between unilateral cleft lip and palate with non-cleft individuals using python programming language

Received: 5 February 2026

Accepted: 4 August 2026

Published online: 31 August 2026

Cite this article as: Huqh M.Z.U., Yaacob H.B., Selvaraj S. *et al.* Comparison of mid-palatal suture morphology via suture bone densities between unilateral cleft lip and palate with non-cleft individuals using python programming language. *BMC Oral Health* (2026). https://doi.org/10.1186/s12903-026-09562-2

Mohamed Zahoor Ul Huqh, Hashim Bin Yaacob, Siddharthan Selvaraj, Apitchaya Pruksametanan & Johari Yap Abdullah

Comparison of Mid-Palatal Suture Morphology via Suture Bone Densities between Unilateral Cleft Lip and Palate with Non-Cleft Individuals using Python Programming Language

Mohamed Zahoor Ul Huqh[1]*, Hashim Bin Yaacob[2,3], Siddharthan Selvaraj[3,4]*, Apitchaya Pruksametanan[5] and Johari Yap Abdullah[6,7]

[1] Faculty of Dentistry, SEGi University, Petaling Jaya, Selangor, Malaysia.

[2] Faculty of Dentistry, SEGi University, Kota Damansara, Petaling Jaya, Selangor, Malaysia, hashimyaacob@segi.edu.my

[3] Faculty of Dentistry, University of Puthisastra, Phnom Penh, Cambodia

[4] Department of Dental Research Cell, Dr. D. Y. Patil Dental College & Hospital, Dr. D. Y. Patil Vidyapeeth (Deemed to Be University), Pune, India

[5] Institute of Dentistry, Suranaree University of Technology, Nakhon Ratchasima, Thailand apichaya.p@sut.ac.th

[6] Craniofacial Imaging Laboratory, School of Dental Sciences, Health Campus, Universiti Sains Malaysia, Kubang Kerian, Kota Bharu, Malaysia. johariyap@usm.my

[7] Dental Research Unit, Center for Transdisciplinary Research (CFTR), Saveetha Dental College, Saveetha Institute of Medical and Technical Sciences(SIMATS), Saveetha University, Chennai, Tamil Nadu, India

***Corresponding Authors**

Email: ssiddharthan@puthisastra.edu.kh ; mohamed.zahoor.ul.huqh@segi4u.my

Abstract

Introduction: This study aimed to compare the mid-palatal suture (MPS) bone density between individuals with unilateral cleft lip and palate (UCLP) and non-cleft (NC) controls using cone-beam computed tomography (CBCT) imaging and Python-based computational analysis. We hypothesized that children with UCLP would exhibit significantly lower bone density in the MPS region compared to NC individuals, reflecting defective MPS maturation secondary to the congenital cleft defect and its associated surgical interventions.

Materials and Methods: A retrospective case-control study was carried out. A total of 100 participants were included. Data were collected from the databases of Hospital Universiti Sains Malaysia and Hospital Raja Perempuan Zainab II, respectively. Cone beam computed CT scans of both UCLP and NC patients were used to evaluate MPS maturation phases. The images were analysed using the Romexis software version 3.8.2. Data distribution was assessed using the Shapiro–Wilk test for normality ($p < 0.05$ indicating deviation from normality) and Levene's test for

homogeneity of variances. The group comparisons were conducted using the Mann–Whitney U test.

Results: Significant differences were observed in the means of MPSD1, MPSD2, MPSD3, MPSD4, and MPSD5. In comparison to NC individuals, UCLP children displayed considerably decreased bone densities in the MPS region of the palate. Based on the distribution of the participants across the MPS stages, the highest frequency was noticed in Stage E (37%), followed by Stage D (27%), Stage C (20%), and Stage B (8%).

Conclusions: Children with the UCLP group had lower palatal bone density compared to the NC group, indicating defective MPS fusion. These results highlight the need for individualized treatment planning for orthodontic treatment and maxillary expansion in children with clefts.

Keywords: Mid-palatal suture, bone density, python coding, cleft lip and palate

Introduction

The suture that connects the palatal bone to the left and right maxilla is known as the palatal suture. It is comprised of the transverse palatal suture that creates the boundary between the palatal and maxillary bones, and a mid-palatal suture (MPS) that is located in the middle maxillary region [1]. The morphology and development of MPS were first determined by observation of bone specimens directly [2,3], followed by radiographic investigations [4-6]. In forensic science, the palatal suture serves as an age indicator like the calvarial suture [7,8]. The calvarial and palatal sutures have been shown to have fractal features [9]. The MPS is vital for growth and development [10]. During the developmental stage, palatal shelves emerge from both sides of the maxillary floor and later unite to produce the soft and hard palate [11].

CLP may cause significant alterations in the form and extent of congenital abnormalities [12,13]. The MPS is abnormally lateral to the midline in complete unilateral cleft lip and palate (UCLP), and the cleft side segment has no sutural relationship with the non-cleft (NC) side maxilla. Few studies were conducted to examine whether it was feasible to expand the maxilla before surgery or after alveolar bone grafting (ABG) [14,15]. Clinically, MPS development is significant from an orthodontic perspective. Because maxillary growth failure can lead to common dentofacial anomalies like malocclusion and dental crowding [16,17].

Due to restricted transverse development of the maxillary arch, maxillary expansion is essential [18-20]. Thus, rapid maxillary expansion (RME) is a routine procedure in CLP patients to correct the maxillary and mandibular width discrepancies [21-23]. RME can be achieved successfully

without the need for surgery in children in the pre-adolescent to adolescent age group due to the non-fusion of the mid-palatal suture (MPS). The resistance to expansion increases in adulthood due to the ossification of the circummaxillary and MPS [24].

RME has been shown to enhance nasal width, resistance, and breathing in growing children. Because of the closure of the MPS and the significant buttress of the sphenoid, zygomatic, and nasal bones, RME therapy in adults can present a number of challenges. However, if the degree of closure of the MPS can be precisely determined, the traditional RME method for palate expansion can be employed [25].

It has been proposed that an alveolar cleft encompasses the area corresponding to the tooth bud of the maxillary lateral incisor, inhibiting the formation of an intermaxillary suture in the premaxilla region. Thus, individuals with complete alveolar clefts may have an MPS in the premaxilla. Although there is no consensus on whether the premaxillary suture occurs in cleft patients, investigations confirming the absence of a completely distinct premaxillary suture have been recognized as the "incisive fissure" [26-28]. A thin suture called the incisive suture is located in the anterior region of the premaxilla and embryologically originated from the primitive palate. However, in children with CLP, the palatal suture system is disrupted. Only a limited number of studies have discussed expansion in complete UCLP patients, and the presence or absence of MPS in cleft patients remains controversial [28].

In routine clinical practice, chronological age is a typical predictor used to identify whether traditional non-surgical RME or surgical RME is more appropriate [24]. However, there is no strong agreement between the authors in the literature on the age at which surgical RME should be performed [29].

Authors have demonstrated a selective technique for evaluation of MPS maturation stages using cone beam computed tomography (CBCT), which offers significant diagnostic benefits over conventional imaging methods, allowing for both qualitative and quantitative assessment [30-32]. Hence,

in this study, we have evaluated the MPS morphology, and a comparison was made via its bone densities between UCLP and NC individuals.

Materials and methods

Study design and data collection

This retrospective case-control study was carried out to compare mid-palatal suture grey density values between individuals with unilateral cleft lip and palate (UCLP) and non-cleft (NC) controls. A total of 100 participants (50 UCLP and 50 NC) were included. Data were collected from the databases of Hospital Universiti Sains Malaysia and Hospital Raja Perempuan Zainab II, respectively.

The MPS maturation stages were identified using the CBCT scans of both cleft and NC individuals. The UCLP group included: Children with non-syndromic complete UCLP, Patients who have undergone primary palatoplasty and cheiloplasty. The NC group composed of patients with skeletal or dental malocclusions and the patients whose files are completely accessible in the hospital database.

Individuals with other types of clefts such as bilateral and partial clefts, any patients with associated syndromes, children who have undergone secondary ABG and orthodontic treatment, and blurred CBCT images were excluded from the study.

The data of patients who attended the HUSM and HRPZ-II between July 2011 and May 2021 have been collected. Ethical approval was sought from the Jawatankuasa Etika Penyelidikan Manusia (JEPeM) of Universiti Sains Malaysia (USM) with approved code USM/JEPeM/21080533. For data

from Hospital Raja Perempuan Zainab II (HRPZ II), a registration was obtained from National Medical Research Register from the Medical Research Ethics Committee (MREC), Kementerian Kesihatan Malaysia (KKM), with approved study protocol code NMRR ID-22-00233-NSW (IIR). To access the patient's data, prior permission was taken from the relevant hospital directors.

Sample size calculation and sampling method

Sample size was determined using PS Power and Sample Size software (version 3.1.2). For an independent two-group comparison with $\alpha = 0.05$, a mean difference (δ) of 50.7 grey value units, and a standard deviation (σ) of 89.63 [33], the sample size of 50 participants per group provided a statistical power of 80% (0.80). Although the actual analysis used a non-parametric Mann–Whitney U test due to non-normal data distribution, this power calculation confirms that the study was adequately powered to detect meaningful differences in mid-palatal suture grey values.

The predetermined sample size was 50 UCLP individuals and 50 NC subjects as controls Purposive sampling was carried out. CLP patients' data logs, and CBCT images were retrieved from the HRPZ II hospital database with prior approval from their respective directors. Convenient sample was performed on NC individuals and records was gathered from the database of HUSM's specialist orthodontic clinic.

Data Acquisition

The Planmeca Promax imaging system (Planmeca Oy, Helsinki, Finland) was used to capture the CBCT x-rays with an exposure of 90 kV, 8 mA,

and a field of view up to 17x20 cm for 13-14 seconds with a standard head position in a standing posture. The imaging device examines the patient's head horizontally using a narrow X-ray beam and a low radiation dosage. Fig 1 displays the Planmeca Promax imaging device. A single romexis software version 3.8.2 was used to standardize the measurements, and Fig 2 shows the corresponding measurements taken on a desktop computer in Universiti Sains Malaysia's (USM) digital lab. Cross-sectional images from standardized CBCT in axial slice were utilized to assess the various stages of MPS development.

The categorization provided was used to determine the radiographic phases of the MPS as per the classification described by Angelieri *et al.* [34]. The MPS was divided into five phases i.e. from phase A to phase E based on the presence of intermaxillary bony lines as illustrated in Figures 3(a) and 3(b).

A dataset was generated from the raw data to compare mean bone densities in both the maxillary and palatal areas using the python-comprehensive library version 3.12.5. The coding syntax and analysis has been mentioned in the supplemental file S2.

Data storage

The extracted features were stored in CSV files with the following columns:

- Patient_ID: Unique alphanumeric identifier.

- Group: UCLP or NC.

- MPS Stages: Categorical label (A, B, C, D, or E).

- Bone_Density Measurements: MPSD (1-5) in grey density value (GDV) for maxillary/palatal regions.

- DICOM files were archived securely, and CSV files were stored locally on the USM digital lab workstation for analysis.

Mid-palatal suture bone density (MPSD) measurements

Mid-palatal suture grey density values (GDV) were measured at five standardized locations along the anteroposterior axis of the suture (MPSD1 to MPSD5). Regions of interest (ROIs) were placed consistently by a single calibrated examiner. The MPSD dimensions were measured using Mimics software version 17.0 (Materialize, Leuven, Belgium). To examine the MPS, the CBCT images were rotated in the sagittal slice. A red horizontal line was then placed across the anterior nasal spine (ANS) in relation to the posterior nasal spine (PNS) against the matching vertical line to indicate the MPS on the CBCT images. The pictures were rotated in the sagittal view until the complete orientation was achieved, as shown in Fig. 4, to demonstrate that the midpalatal line crossed the ANS and entered the PNS.

The maxillary region (the palatine process of the maxilla) was divided into three equal parts (M1, M2, and M3), and the palatal region (the horizontal plate of the palatine bone) was divided into two equal parts (P1, P2) on the midsagittal slice that crosses the anterior and posterior nasal spine, as shown in Fig. 5. The mean and SD of the GDV's were then calculated on a sagittal

slice passing through the center of each of these sections using a rectangle ROI at 3 mm in width and along the entire height of the MPS. The color coding was assigned with Mimics' automated function for each measurement as follows:

M1 = Orange color, M2 = Yellow color, M3

= Green color P1 = Light blue color, P2 =

Purple color

The mid-palatal suture was segmented into M1-M3 and P1-P2 using established anatomical landmarks, particularly the transverse palatine suture, which serves as a clear transitional zone between the maxillary and palatal regions.

Our investigation was based on the approach mentioned in a previous study by Abo Samra & Hadad [35, 36]. Starting from the most distal point of the incisive foramen, the average GDV was measured for the MPS areas shown below:

Statistical analysis

Python software version 3.12.5 was used to analyze the collected data for associations linked to UCLP using the integrated defined syntax. The Shapiro-Wilk test for normality ($p < 0.05$ indicates deviation from normality) and Levene's test for homogeneity of variances were used to evaluate the distribution of the data, as shown in Table 1. The comparisons were made between the cleft type and MPSD measurements as displayed in Table 2.

The Mann–Whitney U test was used for group comparisons because the parametric testing assumptions were not fulfilled. Cliff's δ and rank-biserial correlation (r) were used to compute effect sizes, and 95% CI were provided for interpretation.

The intraclass correlation coefficient (ICC) at 95% confidence interval was used to determine the intra and inter-examiner reliability of MPSD measurements in both maxillary and palatal regions. The measurements were repeated twice in a two-week interval to calculate the error in estimates. The ICC test findings demonstrated high reliability between the two assessments in all regions (ICC = 0.80 – 0.99).

Results

Demographic and Clinical characteristics

Demographic and clinical data were collected for all participants. Age, sex, and ethnicity were recorded from patient records. The skeletal malocclusion pattern was classified as Class I, II, or III based on the ANB angle and Wits appraisal using WebCeph software (Assemble Circle Corp, Gyeonggi-do, Republic of Korea). For the UCLP group, details of prior surgical interventions (primary lip repair, primary palate repair, and alveolar bone grafting) were obtained from medical records. The demographic characteristics of the study participants are summarized in Table 3.

The distribution of the sample based on morphological maturation stages has been summarized in Table 4. Stage E had the highest frequency in the study population at 37%, followed by Stage D at 27% and Stage C at 20%. While Stage

B and Stage A had the same frequency of 8%. In the overall sample, 36 out of 100 people had an unfused MPS. The greater incidence of Stage D and Stage E, with 19 and 23% respectively, was found in female children in the age group of 14-16 years, as shown in Table 5.

The coding syntax was used in the Python library for the Mann-Whitney U-test to compare the MPSD between UCLP and NC individuals. Significant differences were observed in the MPSD of both maxillary and palatal regions. The mean GDV of MPSD1-MPSD5 were ($p< 0.05$) and found to be significantly reduced in the UCLP group than the NC group, as shown in Table 6. A Bonferroni correction was applied for multiple comparisons (5 variables). (p-values set at < 0.001). Three decimals were found to be significant.

Data Visualization

Matplotlib was used to generate the box plot and violin plot. A boxplot represents the distribution of a numerical variable over one or more groups. Data visualizations were created in Python to understand group variations in MPSD measurements. These plots not only illustrate distributional disparities but also aid in the understanding of effect sizes.

Boxplot, violin plot, and point plot for measurements on the maxillary region

Violin plots and boxplots were used to show the distribution of MPSD1, MPSD2, and MPSD3 values by cleft type (UCLP vs NC individuals). These visualizations presented the overall spread of data, thus enabling clear group comparisons. The generated plots (violin & box) demonstrate

that the NC group had higher MPSD1, MPSD2, and MPSD3 mean values (560.18, 470.90, 410.33) than the UCLP group (420.9, 350.72, 320.89) with upward-shifted data distributions and a higher median. The point plot with 95%confidence intervals (right) confirms this significant difference, as the NC group means for MPSD1, MPSD2, and MPSD3 are clearly higher than the UCLP group means, as illustrated in Figs 6,7, and 8, respectively.

Boxplot, violin plot, and point plot for measurements on the palatal region

The presented plots (violin and box) indicate that the NC group had higher mean values for MPSD4 and MPSD5 (440.35, 470.64) than the UCLP group (360.53, 365.58), with slightly shifted patterns of data distribution and a higher median. The point plot with 95% confidence intervals (right) verifies this significant difference, as the NC group means for MPSD4 and MPSD5 are certainly higher than the UCLP group means, as shown in Figs 9 and 10, respectively. The median of the MPSD4 and MPSD5 values for the UCLP group for both anterior and posterior palatal regions appears to be lower than NC group. This visual distinction is consistent with the Mann-Whitney U test results obtained in Python, which showed a statistically significant group difference with a small negative effect size (r = -10).

Discussion

The MPS begins to ossify with bony spicules emerging from the suture boundaries and "islands" (masses of acellular tissue and unevenly calcified tissues) in the sutural gap. Spicules form in several locations along the suture, with the number of spicules increasing as the suture matures,

resulting in a large number of scalloped areas that are close together but separated by connective tissue in some places. Then, fusion occurs quickly in the posterior region of the suture, with ossification advancing from posterior to anterior, cortical bone resorption in the sutural ends, and cancellous bone formation [36].

When treating individuals with congenital craniofacial malformations like complete UCLP, the palatal suture system is disturbed embryologically and further altered by early primary cheiloplasty and palatoplasty. The tissue tension and scar contraction caused by these procedures are commonly associated with maxillary transverse deficit, a constricted upper dental arch, and posterior crossbites [37].

In routine clinical orthodontic treatment procedures, choosing the appropriate RME technique which can vary from conventional tooth-borne appliances to miniscrew-assisted rapid maxillary expansion (MARME) or surgically assisted RME has traditionally relied heavily on chronological age. Multiple investigations have confirmed that chronological age is not an accurate predictor of suture maturity due to individual biological variation [38,39].

As an instance, structural interdigitation and partial obliteration of the MPS may vary considerably between adolescence and young adulthood. This variation emphasizes the crucial need for individual anatomical assessment rather than relying solely on age-based milestones to avoid expansion failures and unnecessary treatments involving surgery [40].

RME failure in certain people may be caused by anatomical variances. Although sutural failure is not evaluated in this study, it is important to assess and fully understand the anatomical alterations in MPSD in UCLP patients since sutural expansion failure is frequently observed in teenagers and young adult patients [41]. Because MPS maturation and bone densities alter frequently in such individuals, chronological age cannot be used to predict the outcome of treatment. Thus, an individual assessment of MPS maturation and MPSD is essential before initiating the orthodontic therapy [36,38,42].

Even though the RME protocol has been incredibly successful in everyday clinical practice. Only a few investigations have analyzed treatment-related changes in children with CLP [43-45]. The biomechanical effects that result from RME in CLP patients appear to differ from those reported in individuals without this craniofacial deformity, owing to changes in anatomical features [45, 46].

To overcome chronological age constraints, Angelieri et al. [33] developed a standardized five-stage classification method (Stages A–E) based on axial CBCT slices.

Due to the wide range of anatomical variations in the maxillary arch, numerous maxillary expanders have been developed. A recent study has investigated the impact of non-surgical expanders designed for anterior arch extension, such as the fan-type and inverted mini-Hyrax, connected to a transpalatal arch. Both groups reported significant transverse maxillary

growth, with the maxilla's posterior expansion being larger than its anterior opening. When comparing the mean difference between anterior and posterior locations within the same group, the majority of variables revealed stronger posterior than anterior expansion (p <0.05) [44].

In addition, specific post-expansion measurement evaluation such as monitoring a bone density change via CBCT over 6- to 12-month periods shows that, while dense, mature sutures experience early bone density reductions immediately upon mechanical separation. The younger patients and targeted force vectors through custom-made MARME workflows reveal profound bone regeneration and ultimate structural healing within one year. Using objective data analytics allows clinicians to accurately determine whether an individual presenting with a cleft maxilla has enough structural bone density to withstand non-surgical mechanical separation or if surgical distraction osteogenesis is necessary [40, 47].

Surgical RME is a type of distraction osteogenesis (DO) with predictable and consistent outcomes. It is currently being utilized to treat maxillary hypoplasia. With rapid orthodontic tooth movement and vertical alveolar augmentation, DO can also help individuals with secondary palatal clefts. If an osteotomized dental arch can be relocated to a new position without complications, it will avoid the need for a subsequent bone transplant to the cleft alveolus in cleft patients. It will also help prevent dentoalveolar anomalies by approaching the originally formed alveolar bone and gingiva [48]. As a consequence, non-surgical extension of the MPS in adults is

quite challenging, and RME may only be performed surgically via MPS osteotomy and corticotomy of the adjacent skeletal tissue. However, the traditional RME technique for palate expansion can be applied if the degree of closure of the MPS can be precisely ascertained. At the ages of 14–15 for girls and 15–16 for males, the MPS begins to close [49].

In this study, we have assessed the MPS maturation stages and compared their bone densities between UCLP and NC individuals using the Mann-Whitney U-test with Python coding syntax. Furthermore, Python enables the creation of a highly standardized and systematic pipeline for CBCT image processing, resulting in consistent grey density measurements across multiple slices while eliminating operator-dependent variability. The seamless integration of all analytical procedures, including data cleansing, assumption testing, non-parametric analysis, effect size calculation, and visualization, into a single scripting environment significantly boosted workflow efficiency. Our findings revealed a statistically significant decrease in mean grey density GDVs across all five anatomical segments (MPSD1 to MPSD5) in the UCLP group compared to NC subjects. This systemic decrease in bone density reveals an altered microarchitecture and defective fusion process related to cleft palate.

As per Angelieri et al. [33], the stages of MPS maturation suggest that the MPS fusion in the palatal area begins in stage D and is completely fused in stage E. These findings are consistent with our study results. The more frequently observed stages in this research were E (37%) and D (27%),

followed by stage C (20%). The less frequently observed stages were A (8%) and B (8%), respectively. The open sutures were found in all three remaining stages, A, B, and C, respectively.

The box, violin, and point plots for MPSD measurements in both the maxillary and palatal regions consistently show that, in comparison to the NC group, the mean bone density values of the UCLP group were typically decreased. This may suggest that there is a significant variation exists between the two groups with respect to the measured attributes. The violin plots used in our study depict the distribution of a dataset and indicate the probability density at various levels. A violin plot can be useful for illustrating the shape of the data distribution in addition to the information given by a box plot. The location of the dot in a point plot indicates the central tendency of a numerical variable, while error bars show some degree of disparity around that estimate.

The measurements of MPSD in the present investigation revealed that the palatal region has exhibited lower bone densities in children with UCLP, in contrast to individuals with NC. Moreover, our findings are consistent with the study by Moscarino et al. [50], who assessed palatal bone thickness and soft tissue architecture in cleft patients and reported that the anterior palate region opposite the cleft side has the greatest structural bone thickness. This spatial distribution has important clinical implications: while the posterior and cleft-adjacent zones have reduced bone density, the denser non-cleft anterior segment is an ideal anatomical site for orthodontic

mini-implant anchoring or temporary anchorage devices (TADs), allowing for stable expansion protocols without compromising the fragile alveolar fragments.

On the contrary, the bone and soft tissue ratios were found to be highest in the anterior region and lowest in the posterior region among NC people [51]. Evaluating MPS bone via grey densities in different regions of the maxilla and palate may shed light on different skeletal patterns, age groups, and genders. These metrics serve as an additional parameter for clinical assessments rather than acting as a direct guide for treatment decisions.

Conclusion

Children with UCLP showed altered MPS maturation, as seen by lower palatal bone density compared to their NC counterparts. These findings emphasize the necessity of personalized treatment planning for maxillary expansion and orthodontic interventions in cleft children. In these instances, RME may be considered as a viable treatment option to correct the transverse maxillary deficiencies with time and techniques corresponding to the MPS maturation stage determined by CBCT evaluation.

The frequency of MPS maturation was found to be high in the 14-16 age group. The highest percentages of D (27%) and E (37%) MPS maturation stages, respectively, were found in female children. The greater number of ossifications was seen in stages D and E, respectively. It has been proposed that bone densities will be high in young children as their age advances.

Python software was used for statistical analysis, including libraries for data processing, testing, and data visualization. Python enables computational efficiency by integrating with various higher-level libraries to deliver optimized performance execution.

Limitations of the study

The present investigation cannot determine whether the MPS morphology in individuals with different types of clefts will have similar outcomes. Furthermore, our study sample included only Malay and Chinese children of Malaysian descent. It is crucial to note that the findings of the study may not be generalizable to other ethnic or racial groups.

Since growth status and age quartiles were not assessed in this study, it is suggested that future research must incorporate an assessment of development stages utilizing the Cervical Vertebral Maturation Index (CVMI). In addition, longitudinal multi-center trials should be conducted to assess any substantial differences in age-related characteristics.

Ethics approval and consent to participate:

This study was granted approval by the Human Research Ethics Committee of Universiti Sains Malaysia (approval number, USM/JEPeM/1080533 dated 24th November 2021) and carried out in compliance with the Declaration of Helsinki. Since this study only used secondary data gathered from the HUSM and HRPZ II patient records, patient consent was waived off by Human Research Ethics Committee of Universiti Sains Malaysia.

Funding

The author(s) declare that financial support was received for the research and/or publication of this article. This study was funded by TDC holdings Sdn Bhd through Universiti Sains Malaysia with grant no. 304.PPSG.6150194/T152.

Acknowledgment

The authors would like to thank the Department of Craniofacial Sciences and Orthodontic Unit, School of Dental Sciences at University Sains Malaysia, Health Campus, Kelantan, Malaysia.

Data availability:

All data generated or analysed during this study are included in supplementary information file S1.

Disclosure statement:

Authors declare there is no potential conflict of interest.

Author Contributions:

MZUH: Conceptualization, Methodology, Investigation, Formal analysis, Writing-Original draft preparation. HBY: Writing-Review & Editing, SS: Methodology, Data analysis, Writing-Review & Editing, AP: Writing-Review & Editing, JYA: Project Administration, Supervision, Funding Acquisition, Conceptualization, Writing-Review & Editing.

References

1. Drake RL, Vogl AW, Mitchell AW. Gray's Anatomy for Students Flash Cards: Gray's Anatomy for Students Flash Cards E-Book. Elsevier; 2019.
2. Wood JK. Direction and type of the transverse palatine suture and its relation to the form of the hard palate. Am J Phys Anthropol. 1949;7(3):385-99, incl 2 pl.
3. Del Santo Júnior M, Minarelli AM, Liberti EA. Morphological aspects of the mid- palatal suture in the human foetus: a light and scanning electron microscopy study. Eur J Orthod. 1998;20(1):93-9.
4. Thadani M, Shenoy U, Patle B, Kalra A, Goel S, Toshinawal N. Midpalatal Suture Ossification and Skeletal Maturation: A

Comparative Computerized Tomographic Scan and Roentgenographic Study. J. Indian Acad. Oral Med. Radiol.2010;22:81- 7.

5. Fricke-Zech S, Gruber RM, Dullin C, Zapf A, Kramer FJ, Kubein-Meesenburg D, et al. Measurement of the midpalatal suture width. Angle Orthod. 2012;82(1):145- 50.
6. Betlej A, Gandhi V, Upadhyay M, Allareddy V, Tadinada A, Yadav S. Variability of the maxillary suture maturation and density in the subjects with different sex and growth status. Clin Anat. 2021;34(3):357-64.
7. Beauthier JP, Lefevre P, Meunier M, Orban R, Polet C, Werquin JP, et al. Palatine sutures as age indicator: a controlled study in the elderly. J Forensic Sci. 2010;55(1):153-8.
8. Lynnerup N, Jacobsen JC. Brief communication: age and fractal dimensions of human sagittal and coronal sutures. Am J Phys Anthropol. 2003;121(4):332-6.
9. Kwak KH, Kim SS, Kim YI, Kim YD. Quantitative evaluation of midpalatal suture maturation via fractal analysis. Korean J Orthod. 2016;46(5):323-30.
10. Cohen, M. Craniosynostosis: Diagnosis, Evaluation, and Management 2nd edn. Oxford University Press, 2000.
11. Latham RA. The development, structure and growth pattern of the human mid- palatal suture. J Anat. 1971;108(Pt 1):31-41.
12. Chawla, O., Deacon, S. A., Ireland, A. J. & Sandy, J. R. Cleft lip and palate at a glance. Orthod Update, 8(3), 78-84.
13. Yılmaz HN, Özbilen E, Üstün T. The Prevalence of Cleft Lip and Palate Patients: A Single-Center Experience for 17 Years. Turk J Orthod. 2019;32(3):139-44.
14. Cavassan Ade O, de Albuquerque MD, Filho LC. Rapid maxillary expansion after secondary alveolar bone graft in a patient with bilateral cleft lip and palate. Cleft Palate Craniofac J. 2004;41(3):332-9.
15. da Silva Filho OG, Boiani E, de Oliveira Cavassan A, Santamaria M, Jr. Rapid maxillary expansion after secondary alveolar bone grafting in patients with alveolar cleft. Cleft Palate Craniofac J. 2009;46(3):331-8.
16. Proffitt W, Fields H, Larson B, Sarver D. Contemporary orthodontics. 6th Edition. Mosby, Inc; 2018.
17. Shibusawa N, Endo Y, Morimoto N, Takahashi I, Miura T. Mathematical modelling of palatal suture pattern formation: morphological differences between sagittal and palatal sutures. Sci Rep. 2021;11(1):8995.

18. Yang CJ, Pan XG, Qian YF, Wang GM. Impact of rapid maxillary expansion in unilateral cleft lip and palate patients after secondary alveolar bone grafting: review and case report. Oral Surg Oral Med Oral Pathol Oral Radiol. 2012;114(1):e25-30.
19. Thompson JR. The cleft lip and palate problem. Angle Orthod. 1952;22(3):137- 41.
20. Ferguson MWJ. Development of the Face and Palate. Cleft Palate Craniofac J. 1995;32(6):522-3.
21. Lypka M, Yen S, Urata M, Hammoudeh J. Solving convergent vector problems with internal maxillary distractors through the use of a fixed rapid palatal expander. J Oral Maxillofac Surg. 2012;70(7):e428-30.
22. Holberg C, Holberg N, Schwenzer K, Wichelhaus A, Rudzki-Janson I. Biomechanical analysis of maxillary expansion in CLP patients. Angle Orthod. 2007;77(2):280-7.
23. Gautam P, Zhao L, Patel P. Biomechanical response of the maxillofacial skeleton to transpalatal orthopedic force in a unilateral palatal cleft. Angle Orthod. 2011;81(3):503-9.
24. Celebi F, Akbulut S. Relationship between the position of maxilla and rapid maxillary expansion failure. South European Journal of Orthodontics and Dentofacial Research. 2020;7(2):49-54.
25. Doruk, C., Sökücü, O., Sezer, H., & Canbay, E. I. (2004). Evaluation of nasal airway resistance during rapid maxillary expansion using acoustic rhinometry. Eur J Orthod, 26(4), 397-401.
26. Wood NK, Wragg LE, Stuteville OH, Oglesby RJ. Osteogenesis of the human upper jaw: proof of the non-existence of a separate premaxillary centre. Arch Oral Biol. 1969;14(11):1331-9.
27. Behrents RG, Harris EF. The premaxillary-maxillary suture and orthodontic mechanotherapy. Am J Orthod Dentofacial Orthop. 1991;99(1):1-6.
28. Zahra S, Samih H. Absence or Presence of Mid-Palatal Suture in Patients with Complete Unilateral Cleft Lip and Palate, (A Retrospective Study). Egyptian Dental Journal. 2017;63:1155-64.
29. Angelieri F, Franchi L, Cevidanes LH, Bueno-Silva B, McNamara JA, Jr. Prediction of rapid maxillary expansion by assessing the maturation of the midpalatal suture on cone beam CT. Dental Press J Orthod. 2016;21(6):115-25.
30. Kapila SD, Nervina JM. CBCT in orthodontics: assessment of treatment outcomes and indications for its use. Dentomaxillofac Radiol. 2015;44(1):20140282.

31. Jain V, Shyagali TR, Kambalyal P, Rajpara Y, Doshi J. Comparison and evaluation of stresses generated by rapid maxillary expansion and the implant- supported rapid maxillary expansion on the craniofacial structures using finite element method of stress analysis. Prog Orthod. 2017 Dec;18(1):3.
32. Colonna A, Cenedese S, Sartorato F, Spedicato GA, Siciliani G, Lombardo L. Association of the mid-palatal suture morphology to the age and to its density: A CBCT retrospective comparative observational study. Int Orthod. 2021;19(2):235- 42.
33. Bigliazzi, R., Magalhães, A. D. O. S., Magalhães, P. E., de Magalhães Bertoz, A. P., Faltin Jr, K., Arita, E. S., & Bertoz, F. A. (2017). Cone-beam computed tomography evaluation of bone density of midpalatal suture before, after, and during retention of rapid maxillary expansion in growing patients. Journal of the World Federation of Orthodontists, 6(1), 15-19.
34. Angelieri F, Cevidanes LH, Franchi L, Goncalves JR, Benavides E, McNamara JA, Jr. Midpalatal suture maturation: classification method for individual assessment before rapid maxillary expansion. Am J Orthod Dentofacial Orthop. 2013;144(5):759-69.
35. Abo Samra D, Hadad R. Midpalatal suture: evaluation of the morphological maturation stages via bone density. Prog Orthod. 2018;19(1):29.
36. Grunheid, T., Larson, C. E., & Larson, B. E. (2017). Midpalatal suture density ratio: A novel predictor of skeletal response to rapid maxillary expansion. Am J Orthod Dentofacial Orthop, 151(2), 267-276.
37. Gao, L., Chen, Z., Zang, L., Sun, Z., Wang, Q., & Yu, G. (2022). Midpalatal Suture CBCT Image Quantitive Characteristics Analysis Based on Machine Learning Algorithm Construction and Optimization. Bioengineering (Basel, Switzerland), 9(7), 316.
38. Georgiadis, T., Angelopoulos, C., Papadopoulos, M. A., & Kolokitha, O.-E. (2023). Three-Dimensional Cone-Beam Computed Tomography Evaluation of Changes in Naso-Maxillary Complex Associated with Rapid Palatal Expansion. Diagnostics, 13(7).
39. Boggio A, Fiorillo G, Razzani E, Manes Gravina B, Mandelli G, Vinci R, Castellana F and Gastaldi G (2026) A new CBCT evaluation for individual assessment of midpalatal suture maturation: a retrospective analysis. Front. Oral Health 6:1630883.

40. Thi Hong Thuy, P., Viet, H., Thu Trang, P., Phuong Linh, D., & Viet Anh, N. (2025). Midpalatal suture bone regeneration following customized miniscrew-assisted rapid palatal expansion in nongrowing patients: A retrospective observational study. Medicine, 104(41), e44624.
41. Chae JM, Rogowski L, Mandair S, Bay RC, Park JH. A CBCT Evaluation of Midpalatal Bone Density in Various Skeletal Patterns. Sensors (Basel). 2021;21(23).
42. Isfeld, D., Lagravere, M., Leon-Salazar, V., & Flores-Mir, C. (2017). Novel methodologies and technologies to assess mid-palatal suture maturation: a systematic review. Head Face Med, 13(1), 13.
43. Tindlund, R. S., Rygh, P., & Bøe, O. E. (1993). Intercanine widening and sagittal effect of maxillary transverse expansion in patients with cleft lip and palate during the deciduous and mixed dentitions. *Cleft Palate Craniofac J*, ***30*****(2)**, 195-207.
44. Figueiredo, D. S., Cardinal, L., Bartolomeo, F. U., Palomo, J. M., Horta, M. C., Andrade, I., Jr., & Oliveira, D. D. (2016). Effects of rapid maxillary expansion in cleft patients resulting from the use of two different expanders. Dental Press J Orthod, 21(6), 82-90.
45. Figueiredo, D. S., Bartolomeo, F. U., Romualdo, C. R., Palomo, J. M., Horta, M. C., Andrade, I., Jr., & Oliveira, D. D. (2014). Dentoskeletal effects of 3 maxillary expanders in patients with clefts: A cone-beam computed tomography study. Am J Orthod Dentofacial Orthop, 146(1), 73-81.
46. Pan, X., Qian, Y., Yu, J., Wang, D., Tang, Y., & Shen, G. (2007). Biomechanical effects of rapid palatal expansion on the craniofacial skeleton with cleft palate: a three-dimensional finite element analysis. *Cleft Palate Craniofac J*, ***44*****(2)**, 149-154.
47. Nik Ravesh, M., Ameli, N., Lagravere Vich, M., & Lai, H. (2025). Automated classification of midpalatal suture maturation using 2D convolutional neural networks on CBCT scans. Frontiers in dental medicine, 6, 1583455.
48. Chul Tae, K., S. Ging Gong, S. Ki Min and S. Whan Oh (2003). "Use of Distraction Osteogenesis in Cleft Palate Patients." Angle Orthod, 73(5), 602-607.
49. Kwak, K. H., Kim, S. S., Kim, Y. I., & Kim, Y. D. (2016). Quantitative evaluation of midpalatal suture maturation via fractal analysis. Korean J Orthod, 46(5), 323-330.

50. Moscarino S, Scholz J, Bastian A, Knaup I, Wolf M. Bone and soft tissue palatal morphology and potential anchorage sides in cleft palate patients. Ann Anat. 2019;224:41-6.
51. Steegman, R. M., Klein Meulekamp, A. F., Renkema, A. M., Janssen, K. I., Kuijpers-Jagtman, A. M., & Ren, Y. (2024). Three-Dimensional Cone Beam Computed Tomography (CBCT)-Derived Soft Tissue Changes in Patients with Unilateral Cleft Lip, Alveolus, and Palate with Midfacial Deficiency after 1.5 Years of Bone-Anchored Maxillary Protraction. Journal of clinical medicine, 13(10), 2890.

Fig. 1 Planmeca Promax 3D S/L (TPK 355382; Planmeca Oy, Helsinki, Finland).

d on a desktop computer for measurements.

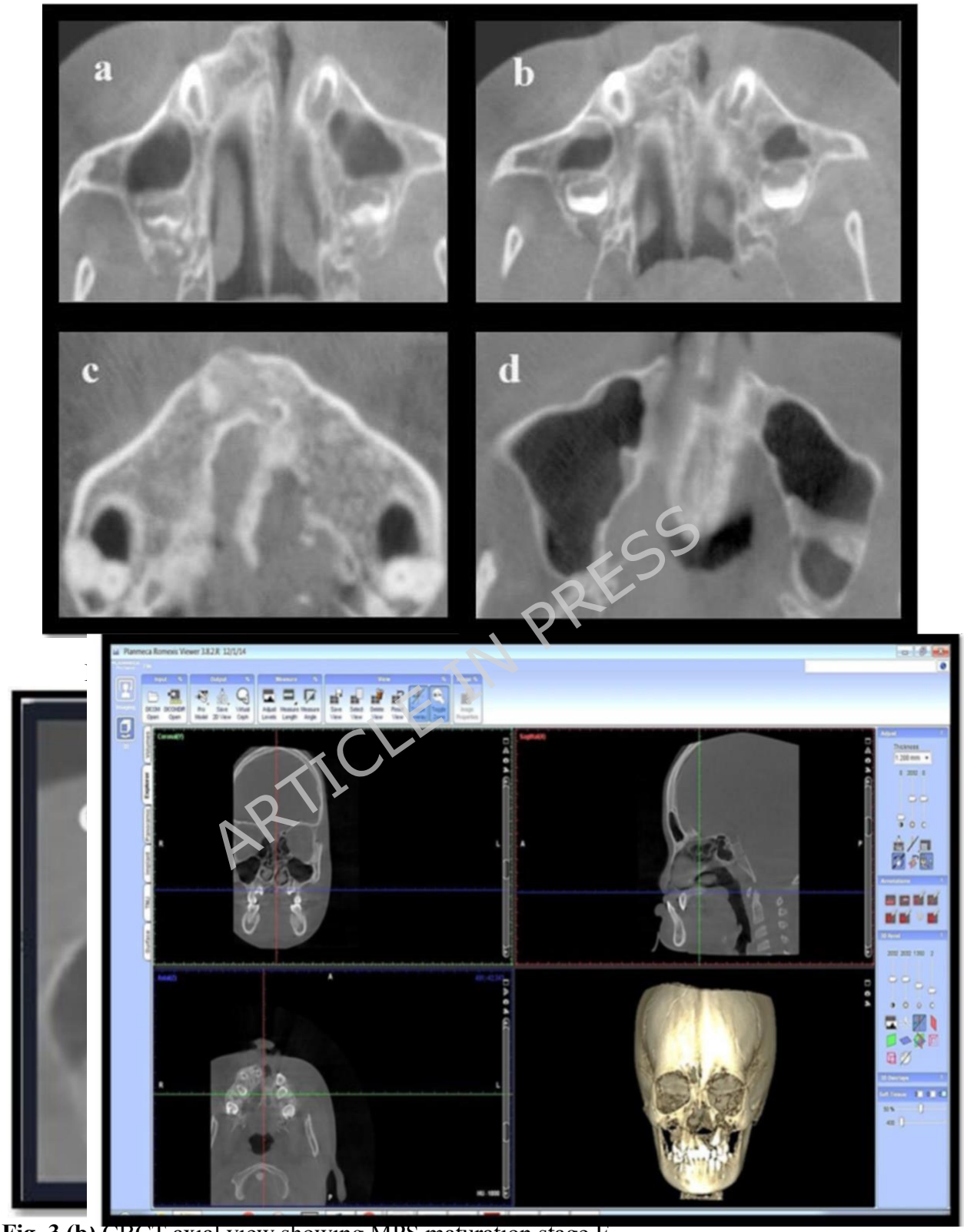

Fig. 3 (b) CBCT axial view showing MPS maturation stage E.

Fig. 4 Complete orientation of the midpalatal suture on CBCT image.

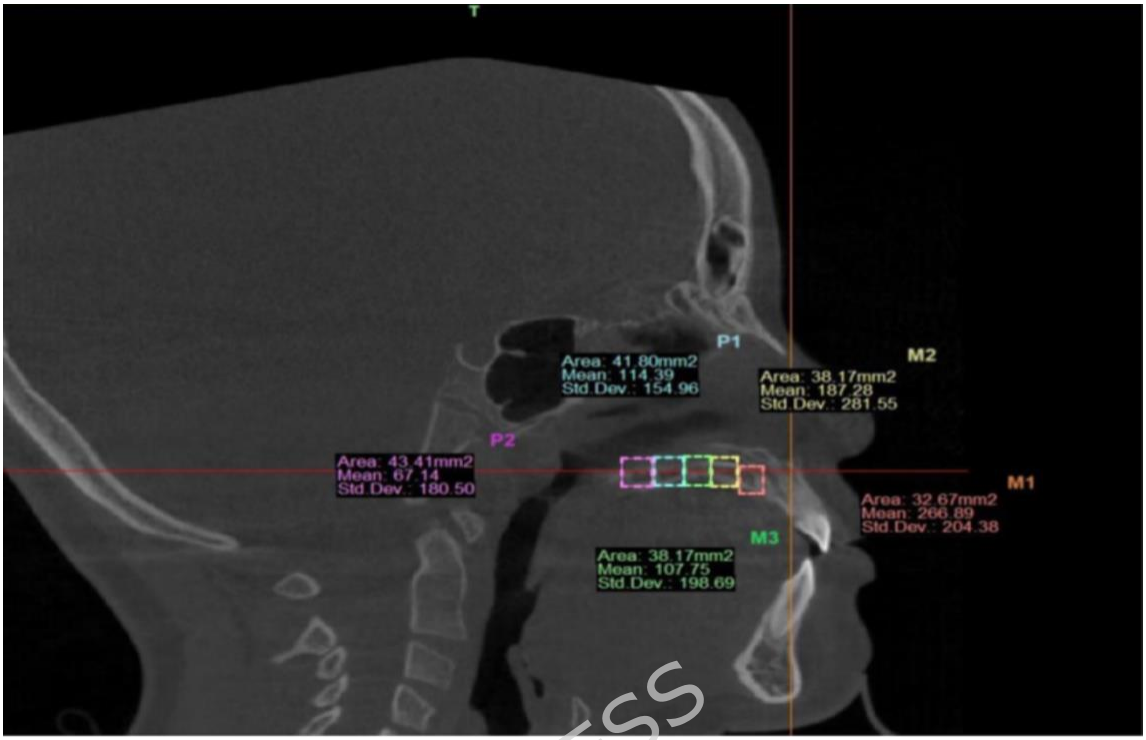

Fig. 5 The maxillary region is divided into three equal parts (M1, M2, and M3), while the palatal region is divided into two equal parts.

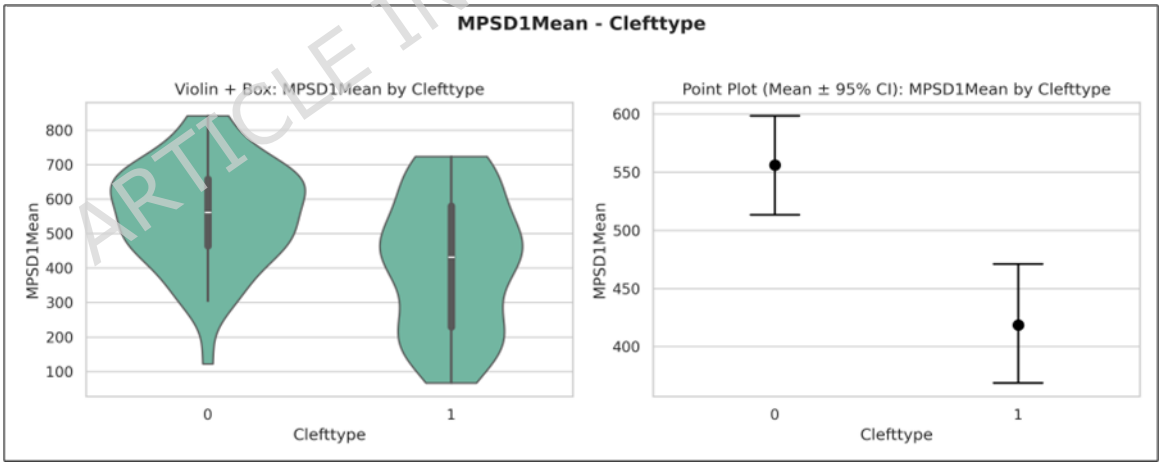

Fig. 6 MPSD1 mean distribution and comparability by cleft type. 0 indicates NC, whereas 1 indicates the UCLP group. The violin + boxplot (left) shows the greater mean values in the NC group compared to the UCLP group. The point plot at 95% CI CS (right) shows the difference in mean values between the two groups.

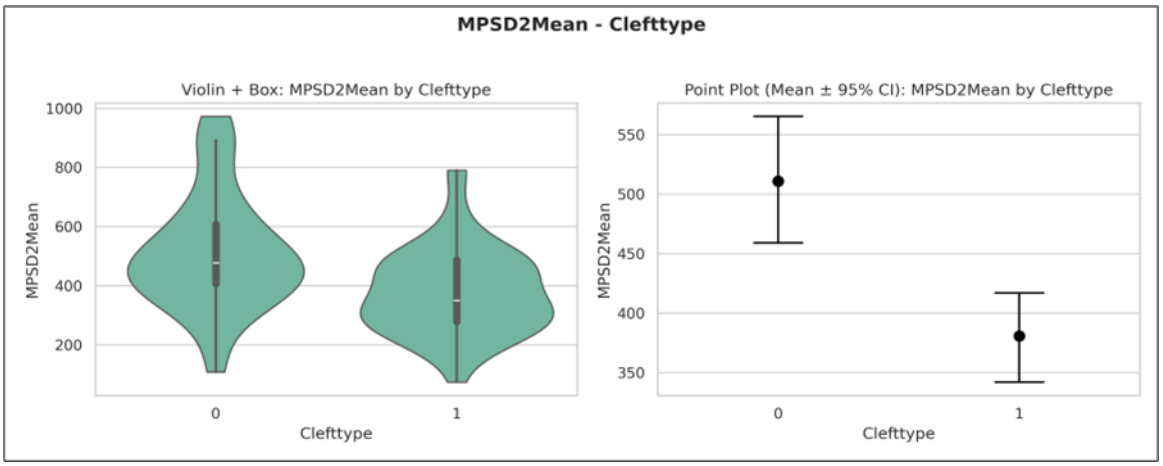

Fig. 7 MPSD2 mean distribution and comparability by cleft type. 0 indicates NC, whereas 1 indicates the UCLP faction. The violin + boxplot (left) demonstrates that the NC group has a higher mean and wider range of values than the UCLP group. The point plot at 95% CI (right) confirms the difference in mean values between the two groups.

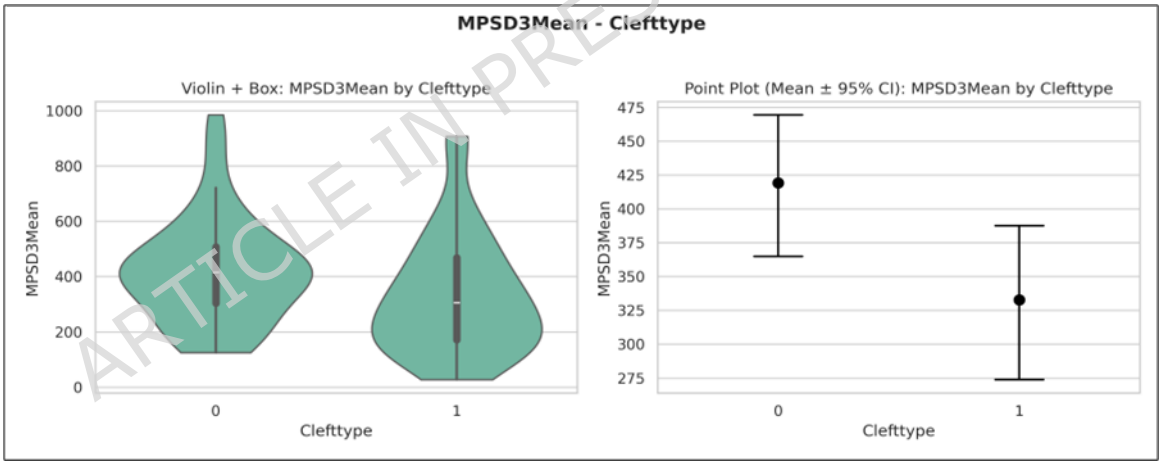

Fig. 8 MPSD3 mean distribution and comparability by cleft type. 0 indicates NC, whereas 1 indicates the UCLP group. The violin and boxplot (left) show that the NC group has a higher mean and greater range of values than the UCLP group. The point plot at 95% CI (right) confirms the difference in mean values between the two groups.

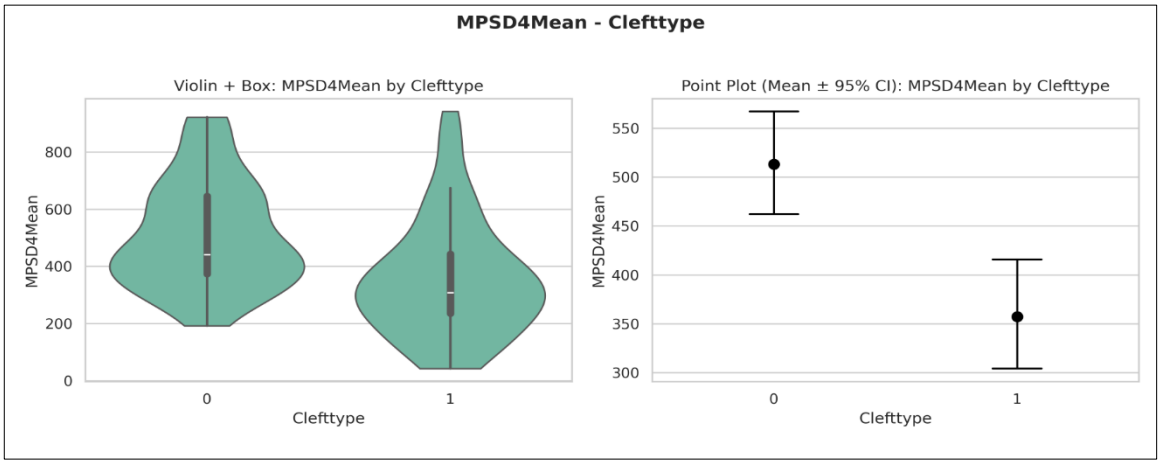

Fig. 9 MPSD4 mean distribution and group comparison by cleft type. 0 represents NC and 1 represents the UCLP group. The violin + boxplot (left) reveals that the NC group has a higher mean and broader range of values in NC group than the UCLP group. The point plot at 95% CI (right) affirms the skewed distribution in mean values between the two groups.

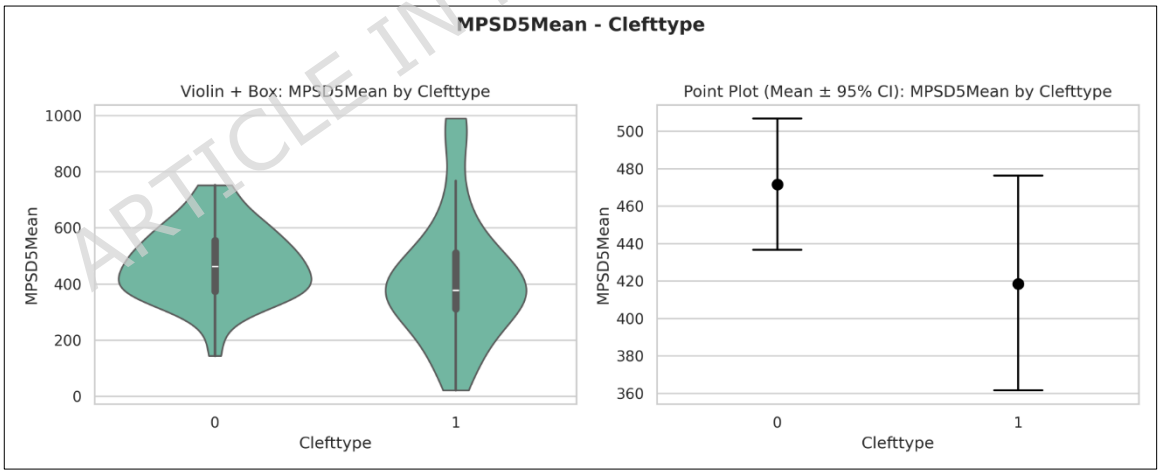

Fig. 10 MPSD5 mean distribution and comparability by cleft type. The violin and boxplot (left) reveal that both groups (UCLP and NC) have a wide distribution, with more variability in the NC group. The point plot (right) clearly shows the difference between the two groups.

Tables

Table 1. Results of the Shapiro-Wilk test and Levene's test for comparison between the gender and measurement variables

Measurement Variables	Shapiro–Wilk test (Normality)				Levene's test (Equality of Variances)	
	Male		Female			
	W	*p*-value	W	*p*-value	F-Statistics	*p-value*
MPSD1Mean	0.932	0.003	0.974	0.436	3.755	0.056
MPSD2Mean	0.935	0.004	0.927	0.009	0.506	0.479
MPSD3Mean	0.965	0.099	0.921	0.006	2.145	0.146
MPSD4Mean	0.955	0.033	0.958	0.118	6.036	0.016
MPSD5Mean	0.954	0.029	0.941	0.028	0.769	0.383

Shapiro-Wilk test: normality assumption is not fulfilled, W=test statistic, p-value < 0.05 Significant.
Levene's test: p-value >0.05 represents equal variances, F-statistics = ratio of variances between the groups.

Table 2. Results of the Shapiro-Wilk test and Levene's test for comparison between the cleft type and measurement variables

Measurement Variables	Shapiro–Wilk test (Normality)				Levene's test (Equality of Variances)	
	UCLP		NC			
	W	*p*-value	W	*p*-value	F-Statistics	*p-value*
MPSD1Mean	0.949	0.030	0.977	0.439	3.935	0.050
MPSD2Mean	0.952	0.040	0.937	0.011	0.506	0.479
MPSD3Mean	0.899	0.000	0.941	0.015	0.937	0.335
MPSD4Mean	0.928	0.005	0.932	0.007	0.000	0.991
MPSD5Mean	0.921	0.003	0.984	0.717	4.435	0.038

Shapiro-Wilk test: normality assumption is not fulfilled, W=test statistic, p-value < 0.05 Significant.
Levene's test: p-value >0.05 represents equal variances, F-statistics = ratio of variances between the groups.

Table 3. Demographic and Clinical Characteristics of the Study Participants

Variables	UCLP Mean(SD)	NC Mean(SD)	Frequency (%) UCLP	NC
Age	14.56(1.24)	12.94(2.30)	-	-
Sex				
Male	-	-	29 (58)	14 (28)
Female	-	-	21 (42)	36 (72)
Ethnic group				
Malay	-	-	39 (78)	33 (66)
Chinese	-	-	11 (22)	17 (34)
Malocclusion class				
Class I			4 (8)	10 (20)
Class II			10 (20)	25 (50)
Class III			36 (72)	15 (30)

Table 4. Distribution of MPS maturation stages based on age and gender

Age (years)	Stage A			Stage B			Stage C			Stage D			Stage E		
	M	F	Total	M	F	Total	M	F	Total	M	F	Total	M	F	Total
8-10	2	1	3	1	-	1	3	2	5	-	-	-	-	-	-
11-13	4	1	5	2	5	7	2	1	3	-	-	-	-	-	-
14-16	-	-	-	-	-	-	7	5	12	8	19	27	14	23	37

M=male, F=female

Table 5. Percentage distribution of the study sample based on age, gender, and maturational stages

Age(years)	8-10		11-13		14-16		
Maturation stages	M(%)	F (%)	M(%)	F(%)	M (%)	F (%)	Total
Stage A	2	1	4	1	0	0	8
Stage B	1	0	2	5	0	0	8
Stage C	3	2	2	1	7	5	20
Stage D	0	0	0	0	8	19	27
Stage E	0	0	0	0	14	23	37

M=male, F=female

Table 6. MPSD measurements of the maxillary and palatal region between UCLP and non-cleft individuals

Dependent Variables (GDV)	**UCLP**	**NC**	**U-Statistic**	**Confidence Interval**	***p*-value significant at**	**Bonferroni Values** (significant at *p< 0.001*)
	n=50	**n = 50**		**95% CI**	*< 0.05*	
Maxillary region						
MPSD1	420.90	560.18	1757	[0.194, 0.606]	0.0005	0.0048
MPSD2	350.72	470.90	1782	[0.213, 0.625]	0.0002	0.0025
MPSD3	320.89	410.33	1624	[0.076, 0.504]	0.0100	0.1003
Palatal region						
MPSD4	360.53	440.35	1859	[0.291, 0.661]	0.0001	0.0001
MPSD5	365.58	470.64	1580	[0.038, 0.486]	0.0229	0.0230

GDV = grey density value, Man-Whitney U-test. p-value

significant at < 0.05, Bonferroni correction
Significant at (p< 0.001)